

Hybrid Organic–Inorganic Nanocomposites: Exfoliation of Magadiite Nanolayers in an Elastomeric Epoxy Polymer

Zhen Wang and Thomas J. Pinnavaia*

Department of Chemistry and Center for Fundamental Materials Research,
Michigan State University, East Lansing, Michigan 48824

Received December 2, 1997. Revised Manuscript Received May 5, 1998

A newly developed class of paraffin-like organomagadiite intercalates, interlayered by primary, secondary, tertiary, and quaternary onium ions, has been used to form elastomeric polymer-layered silicate nanocomposites by in situ polymerization during the thermoset process. Depending on the nature of the onium ions, intercalated or exfoliated magadiite nanocomposites were obtained. The exfoliated nanocomposites were typically disordered, but a new type of exfoliated structure also was observed in which the nanolayers were regularly spaced over long distances (e.g., ~ 80 Å Bragg spacings). The tensile properties of the polymer matrix were improved greatly by the reinforcement effect of the silicate nanolayers. Exfoliated silicate nanolayers were more effective than intercalated assemblies of nanolayers in optimizing reinforcement. Interestingly, organomagadiite exfoliation in the rubbery epoxy matrix improves the elongation-at-break while improving tensile strength, which is opposite to the behavior of conventional composites. The tensile properties of the new epoxy–magadiite elastomeric nanocomposites are compared with those for previously reported nanocomposites derived from smectite clays.

Introduction

Nanostructured hybrid organic–inorganic composites have attracted considerable attention from both a fundamental research and applications point of view.^{1–3} In general, composite materials are formed when at least two distinctly dissimilar materials are mixed to form a monolith. The overall properties of a composite material are determined not only by the parent components but also by the composite phase morphology and interfacial properties. A nanocomposite is formed when phase mixing occurs on a nanometer length scale. For conventional composites, phase mixing occurs on a macroscopic (μm) length scale. Nanocomposites usually exhibit improved performance properties compared to conventional composites, owing to their unique phase morphology and improved interfacial properties.⁴

Layered silicate clays⁵ are good candidates for the formation of organic–inorganic nanocomposites, in part, because they have chemically stable siloxane surfaces and a high surface area. They also possess high aspect ratio and high strength, which are very desirable indexes for use as reinforcing agents. More importantly, the rich intercalation chemistry of clay silicate can be used to facilitate exfoliation of silicate nanolayers into the polymer network. Layer exfoliation maximizes interfacial contact between the organic and inorganic phases.^{6–9}

From a structural point of view, two types of polymer–clay nanocomposites are possible.¹⁰ Intercalated nano-

composites are formed when one or a few molecular layers of polymer are inserted into the clay galleries with fixed interlayer spacings. Exfoliated nanocomposites are formed when the silicate nanolayers are individually dispersed in the polymer matrix, the average distance between the segregated layers being dependent on the clay loading. The separation between the exfoliated nanolayers may be uniform (regular) or variable (disordered). Exfoliated nanocomposites show greater phase homogeneity than intercalated nanocomposites. This structural distinction is the primary reason the exfoliated state is effective in improving the performance properties of clay composite materials.

Toyota researchers first demonstrated that organoclays exfoliated in a thermoplastic nylon-6 polymer matrix greatly improved the thermal, mechanical, barrier, and even the flame-retardant properties of the polymer. These composites now are used in under-the-hood applications in the automobile industry.^{11–14} Over the past few years, this revolutionary nanocomposite chemistry has been successfully extended to the other polymer systems, such as polyimide, epoxy, and poly-

(1) Messersmith, P. B.; Stupp, S. I. *J. Mater. Res.* **1992**, *7*, 2599.
(2) Okada, A.; Usuki, A. *Mater. Sci. Eng.* **1995**, *C3*, 109.
(3) Giannelis, E. P. *Adv. Mater.* **1996**, *8*, 29.
(4) Novak, B. M. *Adv. Mater.* **1993**, *5*, 422.
(5) Pinnavaia, T. J. *Science* **1983**, *220*, 365.

(6) Kato, C.; Kuroda, K.; Misawa, M. *Clays Clay Miner.* **1979**, *27*, 129.
(7) Fukushima, Y.; Inagaki, S. *J. Inclusion Phenom.* **1987**, *5*, 473.
(8) Fukushima, Y.; Okada, A.; Kawasumi, M.; Kurauchi, T.; Kamigaito, O. *Clay Miner.* **1988**, *23*, 27.
(9) Shi, H.; Lan, T.; Pinnavaia, T. J. *Chem. Mater.* **1996**, *8*, 1584.
(10) Giannelis, E. P. *JOM* **1992**, *44*, 28.
(11) Usuki, A.; Kawasumi, M.; Kojima, Y.; Okada, A.; Kurauchi, T.; Kamigaito, O. *J. Mater. Res.* **1993**, *8*, 1174.
(12) Usuki, A.; Kojima, Y.; Kawasumi, M.; Okada, A.; Fukushima, Y.; Kurauchi, T.; Kamigaito, O. *J. Mater. Res.* **1993**, *8*, 1179.
(13) Kojima, Y.; Usuki, A.; Kawasumi, M.; Okada, A.; Fukushima, Y.; Kurauchi, T.; Kamigaito, O. *J. Mater. Res.* **1993**, *8*, 1185.
(14) Kojima, Y.; Usuki, A.; Kawasumi, M.; Okada, A.; Kurauchi, T.; Kamigaito, O. *J. Appl. Polym. Sci.* **1993**, *49*, 1259.

siloxane.^{15–18} Among these, the epoxy–clay nanocomposites with a subambient T_g exhibited exceptionally strong reinforcing effects. For instance, 7.5 vol % of the exfoliated 10-Å-thick silicate layers improve the strength of polymer matrix by more than 10-fold.¹⁹ Also, mass transport studies of polyimide–clay nanocomposites revealed a severalfold reduction in the permeability of small gases, e.g., CO₂, O₂, H₂O, and the organic vapor ethyl acetate.^{15,20} More recently, silicate nanolayers have been dispersed in polypropylene^{21,22} and other thermoplastic and thermoset polymers^{2,23–25} suitable for packaging applications.

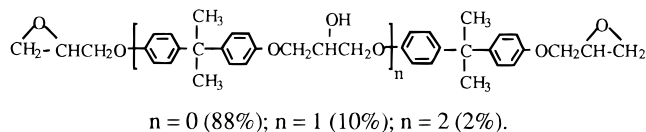
Although considerable research has been conducted on organic–inorganic hybrid composites in which smectite clays are used as reinforcement agents, layered silicic acids^{26–28} have drawn relatively little attention in this field.^{31,32} The family of layered silicic acids includes five members: kanemite (NaHSi₂O₅·*n*H₂O), makatite (Na₂Si₄O₉·*n*H₂O), octosilicate (Na₂Si₈O₁₇·*n*H₂O), magadiite (Na₂Si₁₄O₂₉·*n*H₂O), and kenyaite (Na₂Si₂₀O₄₁·*n*H₂O). They can be easily synthesized by hydrothermal methods, and their acidic analogues can be obtained by proton exchange reaction.^{29,30} Layered silicic acids are potentially good candidates for nanocomposite synthesis, not only because they have platy phase morphology and intercalation chemistry similar to smectite clays but also because they possess high purity and structural properties that are complementary to those of smectite clays.

We have shown recently that magadiite, in addition to forming onium ion intercalates with lateral monolayer and lipid bilayer structures, also forms intercalates in which the alkyl chains adopt a paraffin structure.³² Neither the lateral monolayer or the lipid bilayer structure was suitable for forming exfoliated nanocomposites of epoxy polymers. The lateral monolayer intercalates could not be swelled by the polymer precursors, and an undesirable excess of free amine was needed to form the bilayer structures. However, a paraffin-like derivative could be exfoliated in an epoxy matrix, at least when the galleries were co-occupied by a primary onium ion and the corresponding amine. In the present work, we extend the intercalation chemistry

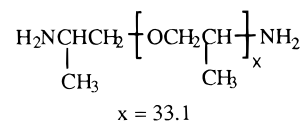
of magadiite to include paraffin structures formed from secondary, tertiary, and quaternary onium ions, in addition to primary onium ions. Also, we report the reinforcement properties of the epoxy nanocomposites formed from these new intercalates, and identify the features of the intercalation chemistry that are most important in determining their tensile behavior.

Experimental Section

Materials. The epoxide resin used for epoxy–magadiite hybrid composite formation was poly(bisphenol A-co-epichlorohydrin) (Shell, EPON 828), with MW ~377:



The curing agent was poly(propylene glycol) bis(2-amino-propyl ether) (Huntsman Chemical, JEFFAMINE D-2000), with MW ~2000:



The above monomers afford a rubber-like epoxy polymer matrix with a subambient T_g of -40 °C. All the other chemicals used in this work were purchased from Aldrich Chemical Co. and used without further purification.

Synthesis of Na⁺–Magadiite. Na⁺–magadiite was synthesized according to the published methods.³³ A suspension of 60.0 g of amorphous silica gel (1.0 mol) in 300 mL of 1.11 M NaOH solution (0.33 mol) was heated at 150 °C for 42 h with stirring in a Teflon-lined stainless steel 1.0 L Parr reactor. The suspension containing Na⁺–magadiite was centrifuged, and the solid product was washed twice with 600 mL of deionized water to remove excess NaOH and air-dried at room temperature.

Synthesis of Organomagadiites. Quaternary alkylammonium-exchanged magadiites were prepared in general by the reaction of 10.0 g of Na⁺–magadiite with 800 mL of 0.117 M CH₃(CH₂)_{*n*-1}N(CH₃)₃⁺Br⁻ (*n* = 12, 16, 18) aqueous solution at 65 °C for 48 h. The products were centrifuged and washed with deionized water until free of Br⁻ and air-dried. For *n* = 12 and 16, the reaction was stopped after 24 h and resumed for an additional 24 h after the mother liquor had been replaced with a fresh solution of onium ions. This treatment could be repeated until free of the Na⁺–magadiite phase, which could be checked by the X-ray diffraction technique.

Primary, secondary, and tertiary long chain alkylammonium-exchanged CH₃(CH₂)₁₇NH_{3-*n*}(CH₃)_{*n*}⁺–magadiites (*n* = 0, 1, 2), designated C18A–, C18A1M–, and C18A2M–magadiite, respectively, were prepared by the following approach. An aqueous suspension containing 15.0 g of Na⁺–magadiite was combined with ethanol:water solution containing 0.121 mol of alkylammonium chloride and 0.020 mol of alkylamine (6:1 molar ratio) to form a suspension in 1.0 L of 1:1 (v/v) ethanol:water total solution. The suspension was stirred at 65 °C for 48 h. The pH of the reaction mixture was in the range 8.0–9.0. The product mixture was added to an equal volume of ethanol and centrifuged. The wet product was washed consecutively with one 750-mL portion of 50% EtOH, two 750-mL portions of 25% EtOH, and then with water until free of Cl⁻ and air-dried. All of the air-dried organomagadiite were ground to a powder with an aggregated particle size smaller than 270 mesh (53 μm) and stored for further use.

(15) Lan, T.; Kaviratna, P. D.; Pinnavaia, T. J. *Chem. Mater.* **1994**, *6*, 573.

(16) Messersmith, P. B.; Giannelis, E. P. *Chem. Mater.* **1994**, *6*, 1719.

(17) Lan, T.; Kaviratna, P. D.; Pinnavaia, T. J. *Chem. Mater.* **1995**, *7*, 2144.

(18) Burnside, S. D.; Giannelis, E. P. *Chem. Mater.* **1995**, *7*, 1597.

(19) Lan, T.; Pinnavaia, T. J. *Chem. Mater.* **1994**, *6*, 2216.

(20) Gu, J. M.S. Thesis, Michigan State University, 1997.

(21) Kurokawa, Y.; Yasuda, H.; Oya, A. *J. Mater. Sci. Lett.* **1996**, *15*, 1481.

(22) Usuki, A.; Kato, M.; Okada, A.; Kurauchi, T. *J. Appl. Polym. Sci.* **1997**, *63*, 137.

(23) Messersmith, P. B.; Giannelis, E. P. *J. Polym. Sci., Part A: Polym. Chem.* **1995**, *33*, 1047.

(24) Pinnavaia, T. J.; Lan, T.; Wang, Z.; Shi, H.; Kaviratna, P. D. *ACS Symp. Ser.* **1996**, *622*, 250.

(25) Vaia, R. A.; Jandt, K. D.; Kramer, E. J.; Giannelis, E. P. *Chem. Mater.* **1996**, *8*, 2628.

(26) Lagaly, G.; Beneke, K.; Weiss, A. *Am. Mineral.* **1975**, *60*, 642.

(27) Beneke, K.; Lagaly, G. *Am. Mineral.* **1977**, *62*, 763.

(28) Beneke, K.; Lagaly, G. *Am. Mineral.* **1983**, *68*, 818.

(29) Rojo, J. M.; Ruiz-Hitzky, E.; Sanz, J. *Inorg. Chem.* **1988**, *27*, 2785.

(30) Pinnavaia, T. J.; Johnson, I. D.; Lipsicas, M. *J. Solid State Chem.* **1986**, *63*, 118.

(31) Sugahara, Y.; Sugimoto, K.; Yanagisawa, T.; Nomizu, Y.; Kuroda, K.; Kato, C. *Yogyo Kyokai Shi* **1987**, *95*, 117.

(32) Wang, Z.; Lan, T.; Pinnavaia, T. J. *Chem. Mater.* **1996**, *8*, 2200.

(33) Fletcher, R. A.; Bibby, D. M. *Clays Clay Miner.* **1987**, *35*, 318.

It is noteworthy that to obtain the C18A, C18A1M and C18A2M paraffin phases ($n = 0, 1, 2$, respectively) it was essential to wash the initial products with carefully controlled amounts of solvent as specified above. Otherwise, most of the organo species was removed from the gallery, resulting in a lateral monolayer structure with a 14.0 Å basal spacing.

Preparation of Epoxy-Magadiite Nanocomposites. Equivalent amounts of epoxide resin and poly(oxypropylene-amine) curing agent were mixed at room temperature for 30 min. The desired amount of organomagadiite was added to the epoxide-poly(oxypropylene-amine) mixture and stirred with a magnetic stirrer for another 60 min. At concentrations below 20 wt % and temperatures between 45 and 75 °C, the mixtures remained pourable. The mixtures were outgassed in a vacuum oven and poured into a stainless steel mold for curing at 75 °C for 3 h and, subsequently, at 125 °C for an additional 3 h.

X-ray Powder Diffraction (XRD). XRD patterns were recorded on a Rigaku rotaflex 200B diffractometer equipped with Cu K α X-ray radiation and a curved crystal graphite monochromator. Samples of epoxy-solvated magadiites or uncured epoxy-magadiite composites were prepared by applying thin films on glass slides. Cured composite specimens were prepared by mounting a flat rectangular sample into an aluminum holder.

Thermal Analysis. Thermogravimetric analyses (TGA) were performed using a Cahn TG System 121 thermogravimetric analyzer. Samples were heated to 750 °C at a heating rate of 5 °C/min under an N₂ atmosphere.

Mechanical Measurements. Tensile testing on individually molded samples was performed at ambient temperature according to ASTM procedure D3039 using a SFM-20 United Testing System. The samples were dog-bone-shaped, 2.5 in. long and 1/8 in. thick. The results for five samples were averaged. The standard deviations of the mean values were typically less than 5%. All curves relating tensile properties to clay loading, as in Figures 5–9, are intended as guides to the eye.

Results and Discussion

Nanocomposite Synthesis. Organic cation intercalation plays an important role in polymer-clay nanocomposite formation by providing a hydrophobic environment for the intragallery adsorption of the polymer precursor. The conversion of a normally hydrophilic inorganic clay to a hydrophobic organoclay also improves the interfacial properties between the organic and inorganic phases when a hydrophobic polymer matrix is involved. Accordingly, our first goal was to synthesize organomagadiites suitable for forming epoxy nanocomposites.

Our initial efforts to form magadiite nanocomposites focused on the intercalation of primary alkylammonium ions, in part, because analogous smectite intercalates are known to exfoliate in thermoset epoxy matrixes. Although Na⁺-magadiite has been reported to intercalate primary alkylammonium ions²⁶ as a lateral monolayer or as a lipid-like bilayer in the presence of a neutral amine, they did not form the desired epoxy nanocomposites. Organo magadiites with a lateral monolayer structure were not swellable by epoxy polymer precursors and were useless in forming nanocomposites. Also, the lipid-like magadiite intercalates contained a relatively high concentration of functional NH groups for epoxide ring opening. This high NH functionality was undesirable, because it led to dangling chain formation and interrupted the epoxy matrix cross-linking.

To reduce the amount of functional NH groups present in the intercalate, we have developed a new

Table 1. Compositions of Organomagadiites with a Paraffin-Like Gallery Structure

material designation	intragallery composition per Si ₁₄ O ₂₉ ²⁻ unit cell
C18A-magadiite	(C ₁₈ H ₃₇ NH ₃ ⁺) _{2.0} (C ₁₈ H ₃₇ NH ₂) _{0.48}
C18A1M-magadiite	C ₁₈ H ₃₇ NH ₂ Me ⁺) _{2.0} (C ₁₈ H ₃₇ NHMe) _{0.30}
C18A2M-magadiite	(C ₁₈ H ₃₇ NHMe ₂ ⁺) _{2.0}
C18A3M-magadiite	(C ₁₈ H ₃₇ NMe ₃ ⁺) _{1.62} Na ⁺ _{0.12} H ⁺ _{0.26}

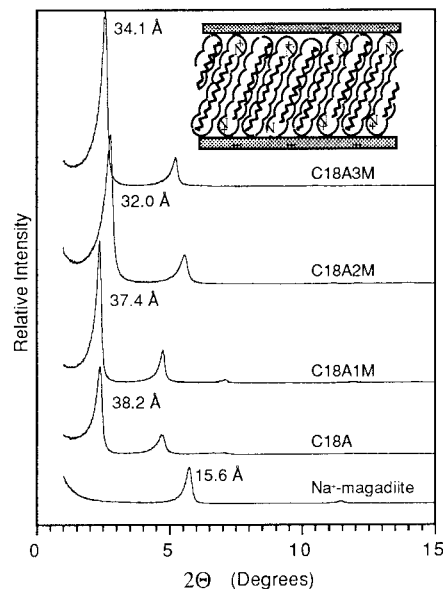


Figure 1. X-ray powder diffraction patterns of air-dried Na⁺-magadiite and organomagadiites with paraffin-like gallery structures (inset). The gallery compositions of the organomagadiites are given in Table 1.

class of paraffin-like intercalated phases of organomagadiite. These paraffin intercalates are prepared by reaction of an aqueous Na⁺-magadiite suspension with a 6:1 molar ratio of long chain primary alkylammonium surfactants of the type CH₃(CH₂)₁₇NH_{3-*n*}(CH₃)_{*n*}⁺ and the corresponding neutral amine in 1:1 (v/v) ethanol:water total solution. This significantly reduces the amount of neutral amine needed to form a hydrophobic intercalate.³² In the present work, we have extended this new synthesis approach to include the preparation of other organomagadiites with paraffin-like gallery structures using long chain secondary and tertiary alkylammonium ions ($n = 1, 2$), as well as primary onium ions ($n = 0$). For comparison purposes, a quaternary alkylammonium ion exchanged magadiite³¹ also was included in the study ($n = 3$).

For convenience, we denote the paraffin-like CH₃(CH₂)₁₇NH_{3-*n*}(CH₃)_{*n*}⁺-magadiite intercalates with $n = 0, 1, 2$, and 3 as C18A-, C18A1M-, C18A2M-, and C18A3M-magadiite, respectively. Table 1 provides their intragallery compositions and basal spacings. A comparison of their XRD patterns is provided in Figure 1. Note that C18A- and C18A1M-magadiite cointercalate 0.48 and 0.30 mol of the corresponding free amine along with 2.0 mol of onium ion per unit cell. For these onium ions with relatively small headgroups, the neutral amine is needed to maintain a paraffin-like structure. Removing the amine by solvent extraction causes the galleries to collapse to a lateral monolayer of onium ions.

All of the paraffin structures described in Table 1 above can be intercalated by epoxide resin at 75 °C to

Table 2. Basal Spacings (Å) for Organomagadiites

material designation	air-dried	epoxy solvated	D-2000 solvated	epoxy and D-2000 solvated
C18A–magadiite	38.2	42.5	63.3	62.7
C18A1M–magadiite	37.4	41.9	52.4	51.4
C18A2M–magadiite	32.0	42.5	32.4	43.1
C18A3M–magadiite	34.1	41.7	34.2	39.1

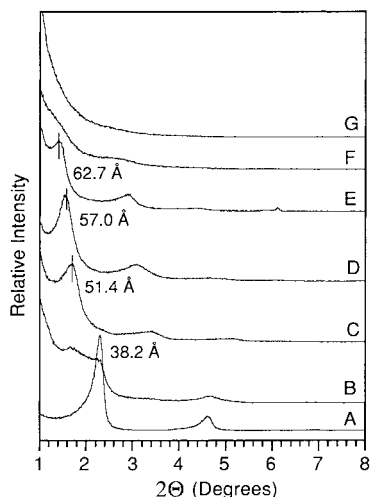


Figure 2. X-ray diffraction patterns of C18A1M–magadiite (15 wt % loading) after reaction with a stoichiometric mixture of epoxide resin (EPON 828) and JEFFAMINE D-2000 curing agent. Reaction conditions were as follows: (A) 25 °C, 30 min; (B) 75 °C, 10 min; (C) 75 °C, 15 min; (D) 75 °C, 30 min; (E) 75 °C, 60 min; (F) 75 °C, 70 min; (G) 75 °C, 90 min.

give derivatives with ~ 42 Å basal spacings (see Table 2). In all cases the onium ions reorient from an inclined angle to a perpendicular orientation to accommodate the resin. C18A– and C18A1M–magadiite also can be intercalated by the poly(oxypropyleneamine) (D-2000) curing agent to form products with spacings of 63.3 and 52.4 Å, respectively. The intercalation of curing agent for these onium ion derivatives may be facilitated by proton transfer between the onium ion and the curing agent. Curing agent intercalation by C18A2M– and C18A3M–magadiite is less favorable, due to the low acidity of the onium ions. Consequently, these latter derivatives imbibe little or no curing agent. Note, however, that a 2:1 stoichiometric mixture of resin and curing agent is effective in swelling all of the organo magadiites.

The intercalation of C18A1M–magadiite by a 2:1 stoichiometric mixture of epoxy resin and curing agent as a function of time was investigated by XRD. As shown by the diffraction patterns in Figure 2 for C18A1M–magadiite, the intercalation process is very slow at room temperature (Figure 2A), because the resin–curing agent mixture is quite viscous and diffusion is slow. Upon heating the system at 75 °C, the C18A1M–magadiite galleries are rapidly solvated, as evidenced by the appearance of a broad diffraction peak at low angle (Figure 2B). This solvated phase continues to swell until a basal spacing of 62.7 Å is reached (cf. Figure 2C–E). At this point in the intercalation process the gallery height corresponds to a bilayer orientation of onium ions with the solvating resin and curing agent accommodated within the bilayer. This 62.7 Å phase is crucial for achieving an exfoliated state of the layer silicates in the finally cured nanocomposite. As the

polymerization of the gallery reagents proceeds with increasing aging time (Figure 2F,G), the galleries continue to expand beyond a bilayer spacing, and the parallel orientation of the nanolayers is lost. The absence of Bragg reflections indicates that the nanolayers are exfoliated in the polymer matrix, but the distance between the nanolayers is not regular. C18A–magadiite exhibited equivalent XRD behavior in forming an exfoliated nanocomposite. Also, we should note that the two-dimensional structure of the magadiite nanolayers is retained in the exfoliated state, as judged by the presence of several strong in-plane peaks in the XRD patterns (not shown).

Figure 3 schematically summarizes the process of nanocomposite formation for the C18A- and C18A1M–magadiite at a reaction temperature of 75 °C. The initial organophilic silicate is easily cointercalated by a stoichiometric ratio of the resin and curing agent at an elevated temperature to form an intercalate with a gallery height equivalent to the thickness expected for a lipid-like bilayer of onium ions (Figure 3B). As the heating is continued, the acidic onium ions catalyze intragallery polymer chain formation at a rate that is competitive with extragallery polymerization. Consequently, the galleries continue to expand in this gel state of polymer (Figure 3C), and the magadiite nanolayers become exfoliated with loss of stacking registry. The relative rates of reagent intercalation, chain formation, and network cross-linking must be controlled to form the gel state and, eventually, the fully cured epoxy-exfoliated magadiite nanocomposite (Figure 3D). On the basis of the relationship between the tensile properties, thermal properties, and the onium ion stoichiometry (see discussion below), the primary and secondary onium ions most likely are incorporated into the polymer matrix. The location of the positive charge associated with the onium ion relative to the silicate surface is not known.

C18A2M– and C18A3M–magadiite behave quite differently from their more acidic C18A and C18A1M analogues in forming epoxy nanocomposites. As shown by the comparison of XRD patterns in Figure 4, the former intercalates afford nanocomposites in which the nanolayers retain their stacking registry, whereas the latter derivatives yield completely exfoliated and disordered (amorphous) nanocomposites. An intercalated nanocomposite was expected for C18A3M–magadiite, because the quaternary alkylammonium ions are non-catalytic and the gallery expansion is determined mainly by the initial loading of resin and curing agent in the gallery. Further expansion of the galleries to the exfoliated state is precluded by the high viscosity and slow diffusion of additional monomers into the gallery. However, C18A2M–magadiite with an intermediate Brønsted acidity forms a new type of magadiite nanocomposite. In this case the nanolayer stacking also is sufficiently regular to give Bragg X-ray scattering along 001, but the interlayer spacing (78.2 Å) is far larger than the value expected for an intercalated nanocomposite with a bilayer of long chain onium ions. Thus, the catalytic polymerization rate appears to be quite uniform from gallery to gallery in this derivative of intermediate acidity, and this leads to an exfoliated state of highly regular periodicity. This regular layer

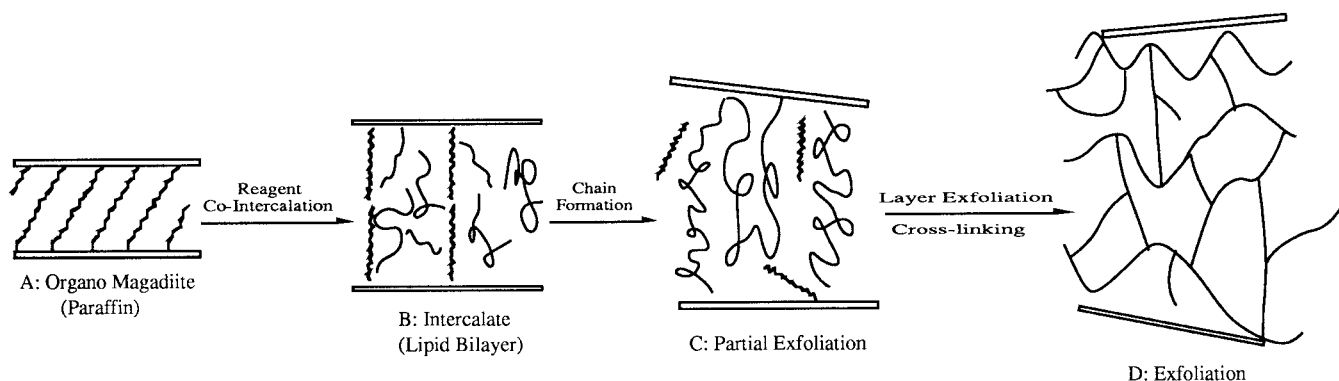


Figure 3. Proposed pathway for the formation of an epoxy-exfoliated magadiite nanocomposite: (A) Initial organomagadiite with a paraffin-like gallery structure of onium ions and neutral amine (see Table 1 for compositions). (B) Reorientation of the alkylammonium ions to a lipid-like bilayer structure to accommodate the cointercalation of epoxide and curing agent. (C) Rapid intragallery formation of a polymer gel and expansion of the gallery height beyond a lipid-like bilayer. (D) Silicate nanolayers are completely exfoliated in a fully cross-linked epoxy polymer network.

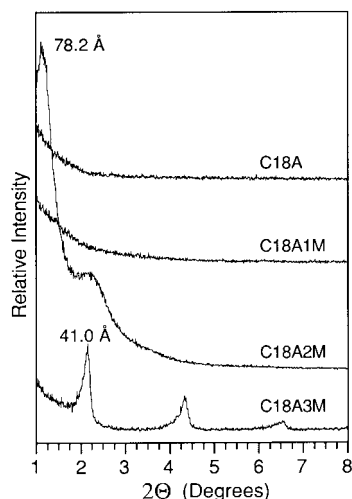


Figure 4. X-ray diffraction patterns of cured epoxy polymer-magadiite nanocomposites prepared from organomagadiites with a paraffin gallery structure (cf. Table 1). The organomagadiite loading is 15 wt % for C18A-magadiite or 20 wt % for C18A1M-, C18A2M-, and C18A3M-magadiite. Polymer curing was carried out at 75 °C for 3 h, followed by 3 h at 125 °C. C18A- and C18A1M-magadiite give highly exfoliated (disordered) nanocomposites ($d > 100$ Å). C18A2M-magadiite also gives an exfoliated nanocomposite, but the layer separation is highly regular ($d = 78$ Å). The quaternary onium ion exchange form, C18A3M-magadiite, forms an intercalated nanocomposite ($d = 41$ Å).

stacking behavior upon exfoliation is unusual, even for smectite clays, having been observed only once for an epoxy nanocomposite prepared from a synthetic fluorohectorite.³⁴

Nanocomposite Properties. A comparison of tensile properties for the epoxy nanocomposites prepared from C18A1M-, C18A2M-, and C18A3M-magadiite is provided in Figure 5. The tensile strengths for all three nanocomposites systems increase with increasing silicate loading. However, the reinforcement benefit is substantially greater for the exfoliated nanocomposites obtained from C18A1M- and C18A2M-magadiite than the intercalated nanocomposites derived from C18A3M-magadiite. Clearly, the tensile properties improve with increasing degree of exfoliation of the nanolayers.

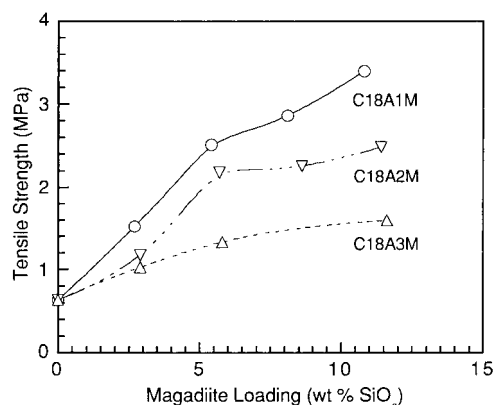


Figure 5. A comparison of the tensile strengths of epoxy nanocomposites prepared from organomagadiites. The magadiite silicate loading (expressed as wt % SiO₂) was determined by calcining the composites in air at 650 °C for 4 h at a heating rate of 2 °C/min. The secondary alkylammonium ion and the free amine content of C18A1M-magadiite was counted as contributing to the stoichiometry for epoxide cross-linking at magadiite loadings > 10 wt %.

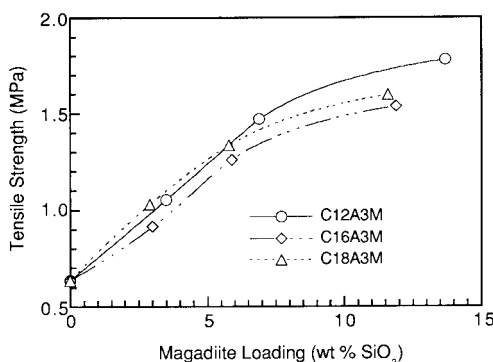


Figure 6. A comparison of the tensile strengths of epoxy-intercalated magadiite nanocomposites prepared from quaternary onium ion-exchange forms of organomagadiites with different alkyl chain lengths. The magadiite silicate loading was determined by calcining the composites in air at 650 °C for 4 h at a heating rate of 2 °C/min.

As illustrated in Figure 6, varying the gallery height of the intercalated nanocomposite from 35.5 to 41.0 Å by changing the chain length of the quaternary onium ion over the range C12 to C18 does not improve substantially the tensile strength of the intercalated nanocomposite. The reinforcement provided by the

(34) Lan, T.; Pinnavaia, T. J. *Mater. Res. Soc. Symp. Proc.* **1996**, *435*, 79.

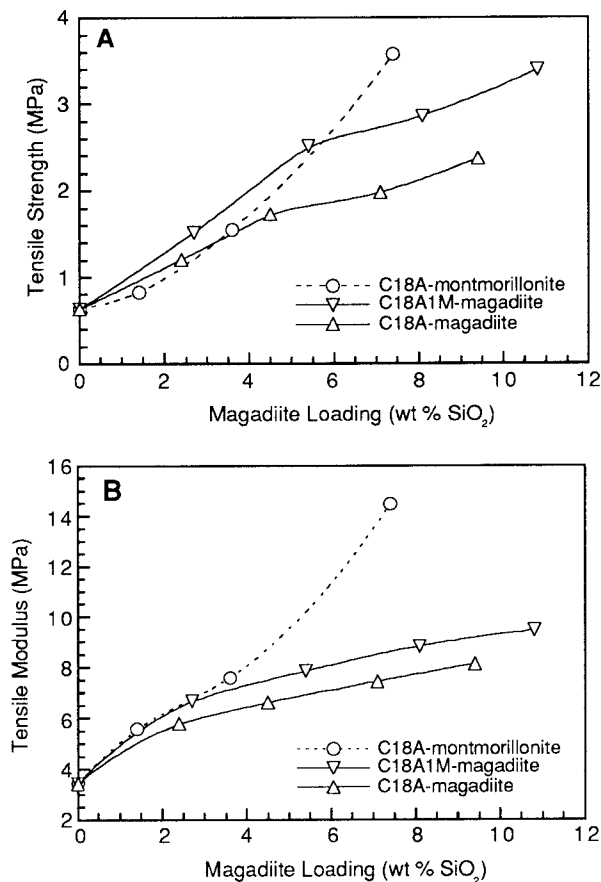


Figure 7. A comparison of (A) the tensile strengths and (B) the tensile moduli for epoxy nanocomposites prepared from C18A- and C18A1M-magadiite and C18A-montmorillonite. The silicate loading was determined by calcining the composites in air at 650 °C for 4 h at a heating rate of 2 °C/min.

intercalated magadiite particles is similar to that provided by conventional (unintercalated) magadiite composites. This suggests that the tensile reinforcement properties provided by the silicate phase do not become additive until the layer separation has reached a separation threshold well beyond an onium ion bilayer, or at least until part of the silicate nanolayers reach that stage.

Figure 7 compares the tensile properties for epoxy-magadiite and epoxy-smectite clay exfoliated nanocomposites. At low silicate loading, the two nanocomposite systems show similar reinforcing performance. At high silicate loadings, however, the epoxy-smectite clay nanocomposites are superior to the magadiite nanocomposites in terms of tensile strength and modulus. The difference in the layer charge density between organomagadiite and montmorillonite contributes to these differences in reinforcement properties. Organomagadiites have a higher layer charge density and, consequently, a higher onium ion and amine content than organomontmorillonites. Our previous studies³² have shown that the gallery alkylammonium-exchanged cations and alkylamine of the organomagadiite are incorporated into the epoxy network to form dangling polymer chains. These dangling chains weaken the polymer matrix by reducing the degree of network cross-linking and compromise the reinforcement effect of silicate layer exfoliation.

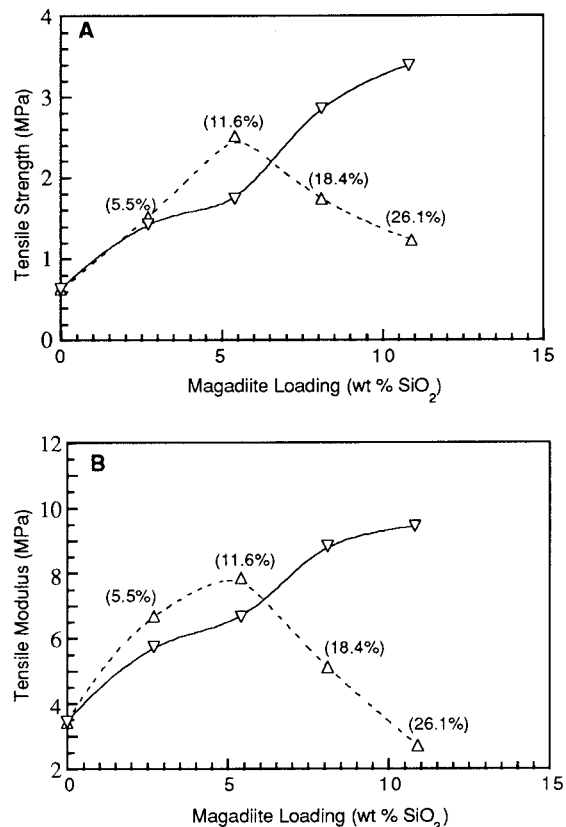


Figure 8. Loading dependence of (A) the tensile strengths and (B) the tensile moduli of epoxy nanocomposites prepared from C18A1M-magadiite. The solid lines are for composites formed by including the onium ion and neutral amine functionality of the organomagadiite as curing agents and reducing the amount of poly(oxypropyleneamine) (D-2000), so that the overall ratio of epoxide to NH bonds is 1:1. The dash lines are for composites formed at an epoxide-D-2000 stoichiometry that disregards the reactivity of the gallery onium ion and amine toward epoxide ring opening. The values in parentheses for the dash curves give the excess NH bond functionality present in the system.

The results in Figure 8 illustrate the effect of dangling chain formation on the tensile properties of epoxy-exfoliated magadiite nanocomposites prepared from C18A1M-magadiite. The dashed line shows the dependence of tensile strength and modulus on loading for composites formed by exfoliating the organosilicate in a matrix containing a stoichiometric ratio of epoxy resin and D-2000 amine curing agent, disregarding the contribution of the gallery onium ion and amine NH groups to the cross-linking stoichiometry. For these compositions the number of dangling chains increases rapidly with increasing organosilicate loading, and maxima are observed in the reinforcement vs loading curves. The solid curves in Figure 8 show the dependence of reinforcement on loading for analogous composites formed under stoichiometric conditions where the amount of D-2000 curing agent is reduced by an amount equivalent to the NH functionality provided by the gallery onium ion and amine. For these latter compositions, there is no excess NH functionality, and the number of dangling chains is minimized. Consequently, reinforcement is optimized.

Interestingly, the introduction of dangling chains through the participation of the gallery onium ions and amines in the matrix curing process affects in the

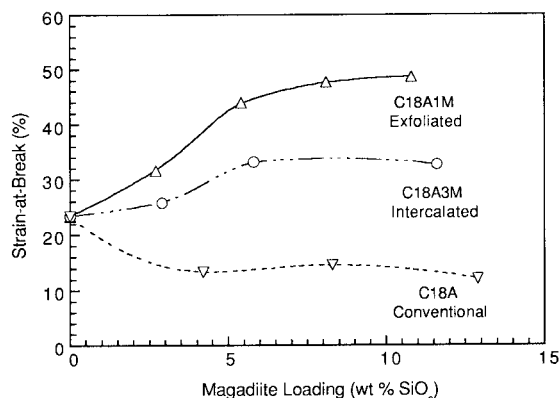


Figure 9. Comparison of the strain-at-break values for an exfoliated epoxy-magadiite nanocomposite prepared from C18A1M-magadiite, an intercalated nanocomposite prepared from C18A3M-magadiite, and a conventional composite prepared from C18A-magadiite with a lateral monolayer structure.³²

elasticity of the polymer in a favor way. As shown in Figure 9, the strain-at-break is substantially increased for exfoliated and intercalated magadiite nanocomposites, whereas conventional (unintercalated) magadiite composites formed from an organomagadiite with a lateral monolayer structure exhibit normal behavior and become less elastic than the pristine polymer. Normally, reinforced composites exhibit a decrease in elasticity relative to the pristine polymer. We attribute the improvement of both elasticity and strength in the case of the exfoliated nanocomposites, in part, to the plasticizing effect of the dangling chains in the polymer matrix and the reinforcement effect of the nanolayers. However, the improvement in elasticity cannot be attributed solely to the presence of dangling chains, because an increase in the strain-at-break also is observed for the intercalated nanocomposites formed from C18A3M-magadiite. In this latter nanocomposite, the quaternary onium ions on the magadiite surface do not contribute to the formation of dangling chains in the polymer matrix.

We also have obtained useful insights into the nature of magadiite nanocomposites from TGA studies of thermal stability. Figure 10 compares the TGA curves for an exfoliated nanocomposite prepared from C18A1M-magadiite and an intercalated nanocomposite prepared from C18A3M-magadiite. Included in the figure are the TGA curves for the pristine organomagadiites. As has been observed previously for nylon 6-exfoliated clay nanocomposites,³⁵ the thermal stability of the polymer matrix is not sacrificed by nanocomposite formation. It is particularly noteworthy, however, that the lower temperature weight loss for the intercalated C18A3M-magadiite nanocomposite is indicative of the decomposition of the quaternary alkylammonium cations on the magadiite basal planes, because an analogous weight loss is observed for pristine C18A3M-magadiite. In comparison, the TGA curve for the exfoliated C18A1M-magadiite nanocomposite does not show a similar low temperature weight loss for the decomposition of surface onium ions, verifying that the secondary onium ions are indeed incorporated into the polymer network.

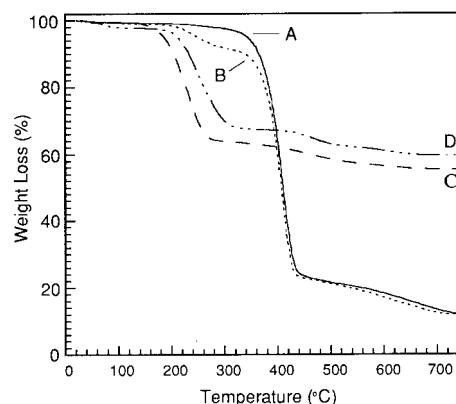


Figure 10. Thermogravimetric analysis curves for epoxy nanocomposites formed from (A) C18A1M-magadiite and (B) C18A3M-magadiite. The loading of organomagadiite was 20 wt % for each epoxy-magadiite nanocomposite. Curves C and D are for the pristine C18A1M- and C18A3M-magadiites, respectively. The analysis was carried out in an N₂ atmosphere at a heating rate of 5 °C/min.

Conclusions

Organomagadiites interlayered by paraffin-like assemblies of primary, secondary, and tertiary alkylammonium ions are highly effective in forming exfoliated nanocomposites with improved tensile properties. Although the primary and secondary onium ion intercalates C18A- and C18A1M-magadiite require the cointercalation of free amine in order to achieve a paraffin-like gallery structure, which increases the NH functionality toward dangling chain formation in the polymer network, these derivatives are far superior to organomagadiites with lipid-like bilayers in forming reinforced nanocomposites. The reinforcement properties of the exfoliated silicate nanolayers can more than compensate for the weakening effect of dangling chain formation, provided that the overall NH functionality present in the reaction system does not greatly exceed the stoichiometric amount needed for curing (e.g., <10%).

The improvement in tensile properties provided by exfoliated magadiite nanolayers is not quite as good as that afforded by exfoliated smectite clays, particularly with regard to tensile modulus at higher loadings. Apparently, the 2:1 sandwiched sheet structure of smectite silicates is stiffer than the silicic acid sheets of magadiite, which are formed by corner sharing of SiO₄ units. However, we have previously pointed out that the nanocomposites formed from exfoliated magadiite layers exhibit better optical transparency than those formed from smectite clays, which may be desirable for certain materials applications. Thus, nanocomposites derived from magadiite complement those obtained from smectite clays with regard to overall materials properties.

Acknowledgment. This work has been supported in part by the following materials research programs at Michigan State University: the Center for Fundamental Materials Research, the Composite Materials and Structure Center, and the NSF State/Industry Cooperative Research Center for Low Cost, High Speed Polymer Composites Processing, with Nanocor, Inc. as the industrial partner.

(35) Gilman, J. W.; Kashiwagi, T.; Lichtenhan, J. D. *Int. SAMPE Symp. Exhib.* **1997**, *42*, 1078.